

Spin configuration of top quark pair production with large extra dimensions at photon-photon colliders

Kang Young Lee^a, Seong Chan Park^b, H. S. Song^{a,b},

JeongHyeon Song^a, and Chaehyun Yu^b

^a*Center for Theoretical Physics, Seoul National University, Seoul 151-742, Korea*

^b*Department of Physics, Seoul National University, Seoul 151-742, Korea*

Abstract

Top quark pair production at photon-photon colliders is studied in low scale quantum gravity scenario. From the dependence of the cross sections on the spin configuration of the top quark and anti-quark, we introduce a new observable, top spin asymmetry. It is shown that there exists a special top spin basis where with the polarized parent electron beams the top spin asymmetry vanishes in the standard model but retains substantial values with the large extra dimension effects. We also present lower bounds of the quantum gravity scale M_S from total cross sections with various combinations of the laser, electron beam, and top quark pair polarizations. The measurements of the top spin state ($t_{\uparrow}\bar{t}_{\downarrow}$) with unpolarized initial beams are shown to be most effective, enhancing by about 5% the M_S bounds with respect to totally unpolarized case.

I. INTRODUCTION

Conventional wisdom is that gravitational interactions suppressed by the Planck scale M_{Pl} are to be neglected at any collider. Recently Arkani-Hamed, Dimopoulos, and Dvali suggested that quantum gravity may become strong at the electroweak scale by introducing large extra dimensions and by confining the standard model (SM) fields to a $(3 + 1)$ -dimensional hypersurface [1]. The observed weakness of macroscopic gravity can be attributed to the largeness of the compactified extra dimensions. Since the fundamental scale M_S can then be around TeV scale, the hierarchy between the electroweak scale and the Planck scale is relieved.

Extra dimension effects are recast in an effective theory valid below the M_S , as a massless graviton propagating in the full $(4 + n)$ -dimensional space is replaced by massive Kaluza-Klein (KK) gravitons propagating in four-dimensional subspace [2]. Since the large phase space of the KK modes enhances the strength of their couplings to the SM particles from $\sim 1/M_{Pl}$ into $\sim 1/M_S$, high energy colliders may provide some distinctive experimental signatures, questioning the above wisdom. Two kinds of collider signals have been studied. Direct signals contain the production of KK states, spin-2 neutral particles [3]. Since they escape collider detectors, the signal is to be recognized as missing energy. In general, the production of KK gravitons is quite sensitive to the number of extra dimensions. Indirect signals with intermediate KK states have less sensitivity to the number of extra dimensions, which are preferable to obtain experimental constraints on the scale M_S [4]. Moreover spin-2 nature of the KK modes leaves characteristic spin configuration of outgoing particles.

In particular, top pair production holds an advantageous position to draw the spin information of the process. Very heavy mass of top quark [5] prompts itself to decay before hadronization, leaving alive the top spin information which can be determined from the angular distribution of its electroweak decay products [6]. Thus the top spin configuration can provide additional observables of new physics, particularly when high

spin particles such as gravitons are involved. At e^+e^- linear colliders (LC), it has been shown that the s -channel diagram mediated by spin-2 KK gravitons significantly modifies the pattern of spin configuration of the top quark and top anti-quark [7].

Photon-photon collisions have been regarded as one of the best alternatives of e^+e^- collisions at LC, where high energy photon beams can be achieved through laser back-scattering of the parent e^+e^- beams. The controllability of the laser and electron beam polarizations provides good opportunities to probe new physics. It is shown that photon colliders are sensitive to the presence of large extra dimensions, yielding higher low bound of the M_S than any other collider [8]. The role of polarizations, however, has been studied only about the laser and parent electron beams.

In this paper we study the large extra dimension effects on the polarizations of top quark pair production at photon colliders, including the top spin configuration which shall be shown to provide a unique channel. From the total cross sections in various top spin bases, we will observe that there is no particular top spin basis where the pattern of the spin configuration is crucially modified by the large extra dimension effects. Instead a new observable, the ‘top spin asymmetry’, is to be introduced. There exists a special spin basis, in particular with polarized electron beams, where this top spin asymmetry vanishes in the SM but has substantial values with low scale quantum gravity effects.

This paper is organized as follows. In Sec. II we present the scattering amplitudes of the $\gamma\gamma \rightarrow t\bar{t}$ process corresponding to the polarizations of initial photons in a general spin basis of the top quark and top anti-quark. The differences from the process $e^+e^- \rightarrow t\bar{t}$ are also discussed. Since photon beams with high energy and high luminosity are to be obtained from e^+e^- LC, we review practical cross sections by taking into account of backward Compton scattering of laser beams from high energy e^+e^- beams. Section III is devoted to the results and discussions. The definition and numerical results of the top spin asymmetry along with an optimal top spin basis shall be given. We also present at 2σ level the lower bound of M_S which top spin information can enhance by a few percents.

Finally Sec. IV deals with our conclusions.

II. FORMALISM

For the process

$$\gamma(k_1, \lambda_1) + \gamma(k_2, \lambda_2) \rightarrow t(p_1, \kappa_1) + \bar{t}(p_2, \kappa_2), \quad (1)$$

there are two types of tree level diagrams in the SM, t -channel and u -channel ones. In Eq. (1), λ_i and κ_i ($i = 1, 2$) denote the polarizations of photons and top quarks, respectively. The effective theory of low scale quantum gravity allows an s -channel diagram mediated by virtual KK graviton modes (see Fig. 1), of which the scattering amplitude is

$$\mathcal{M}_G = -\frac{2s\lambda}{M_S^4} \bar{u}(p_1) \left[(j \cdot \varepsilon_2) \not{\varepsilon}_1 + (j \cdot \varepsilon_1) \not{\varepsilon}_2 + 2\varepsilon_1 \cdot \varepsilon_2 \left(\frac{(j \cdot k_2) \not{k}_1 + (j \cdot k_1) \not{k}_2}{s} - m_t \right) \right] v(p_2), \quad (2)$$

where $j = p_1 - p_2$, and $\varepsilon_i = \varepsilon(k_i)$ ($i = 1, 2$) are the polarization vectors of initial photons. All the ambiguity such as the number of extra dimensions and the compactification models is encoded by order one parameter λ . Hereafter $\lambda = \pm 1$ cases are to be considered, which are sufficient for an estimation of the scale M_S .

Let us review a general spin basis for top quark and top anti-quark [9,10]. Since CP invariance holds in the graviton-mediated diagram as well as in the SM, the spins of the top quark pair lie in the production plane. First defining the spin states of the top quark and anti-quark in their own rest frame, we decompose, respectively, their spins along the reference axes $\hat{\eta}$ and $\hat{\bar{\eta}}$ which are chosen back to back in the zero momentum frame. Thus only one parameter ξ can specify both $\hat{\eta}$ and $\hat{\bar{\eta}}$; the ξ is defined in the top quark rest frame as the clockwise angle between the three-momentum of top anti-quark and the up-state spin of top quark, as depicted in Fig. 2. The usual helicity basis is obtained by setting $\xi = 0$ or π .

When the top quark is emitted in the z -axis, the polarization vectors of initial photons are given by, in the center of momentum (CM) frame with the Coulomb gauge,

$$\varepsilon_1(\pm) = \varepsilon_2(\mp) = \frac{1}{\sqrt{2}}(0, \mp \cos \theta, -i, \mp \sin \theta), \quad (3)$$

where θ is the scattering angle. There is a relation [11], usually being used in the squared amplitudes,

$$\begin{aligned} \varepsilon^i(k, \lambda_1)\varepsilon^{*j}(k, \lambda_2) = \frac{1}{2} \left[(\delta^{ij} - \hat{k}^i\hat{k}^j)\delta_{\lambda_1\lambda_2} - \frac{i}{2}(\lambda_1 + \lambda_2)\epsilon^{ijk}\hat{k}^k \right. \\ \left. - \frac{1}{2}(\lambda_1 - \lambda_2) \left\{ \hat{a}^i(\hat{\mathbf{k}} \times \hat{\mathbf{a}})^j + \hat{a}^j(\hat{\mathbf{k}} \times \hat{\mathbf{a}})^i \right\} \right. \\ \left. + \frac{1}{2}(\lambda_1\lambda_2 - 1) \left\{ \hat{a}^i\hat{a}^j - (\hat{\mathbf{k}} \times \hat{\mathbf{a}})^i(\hat{\mathbf{k}} \times \hat{\mathbf{a}})^j \right\} \right], \end{aligned} \quad (4)$$

where $\hat{\mathbf{a}}$ is an arbitrary unit vector perpendicular to $\hat{\mathbf{k}}$, and $i, j = 1, 2, 3$.

Equation (4) can be applied even in the amplitude level. In the process of Eq. (1), two channels are possible according to the total angular momentum: $J_z = 0$ and $J_z = 2$ states. In the $J_z = 0$ states ($\gamma_R\gamma_R$ or $\gamma_L\gamma_L$), two polarization vectors are related by $\varepsilon_2(+)= -\varepsilon_1^*(+)$, as can be easily seen from Eq. (3). Then the $\varepsilon_1^\mu\varepsilon_2^\nu$ in Eq. (2) can be replaced by

$$\varepsilon_1^i(+1)\varepsilon_2^j(+1) = -\varepsilon^i(k_1, +1)\varepsilon^{*j}(k_1, +1). \quad (5)$$

Note that only the first term in Eq. (4) contributes to the scattering amplitude in Eq. (2) since the last two terms vanish in the case of $\lambda_1 = \lambda_2$, and the anti-symmetric second term does not contribute to the amplitude symmetric under the exchange of two photons. In the CM frame where $\mathbf{j} \cdot \mathbf{k}_1 = -\mathbf{j} \cdot \mathbf{k}_2 = -\mathbf{j} \cdot \mathbf{k}_1$ and $\bar{u}(p_1)\not{k}_1v(p_2) = -\bar{u}(p_1)\not{k}_2v(p_2) = \bar{u}(p_1)\gamma_i v(p_2)k_1^i$, the scattering amplitude mediated by the KK modes vanishes:

$$\mathcal{M}_G^{RR} = \frac{2s\lambda}{M_S^4} \left[\bar{u}\gamma_i v j^j \left(\delta^{ij} - \frac{k_1^i k_1^j}{k_1^0 k_1^0} \right) - \bar{u}\gamma_i v j^i + \frac{\bar{u}\gamma_i v k_1^i (\mathbf{j} \cdot \mathbf{k}_1)}{k_1^0 k_1^0} \right] = 0. \quad (6)$$

Thus the effects of low scale quantum gravity exist only in the $J_z = 2$ channels.

The squared amplitudes for each top spin configuration with the large extra dimension effects are, with $\beta = \sqrt{1 - 4m_t^2/s}$,

$$|\mathcal{M}|^2(\gamma_R\gamma_L \rightarrow t_\uparrow\bar{t}_\uparrow \text{ or } t_\downarrow\bar{t}_\downarrow) = \frac{1}{4}N_c s^2 \beta^2 \sin^2 \theta [D_t + D_u + D_s]^2 F_1^2,$$

$$\begin{aligned}
|\mathcal{M}|^2(\gamma_R\gamma_L \rightarrow t_\uparrow\bar{t}_\downarrow \text{ or } t_\downarrow\bar{t}_\uparrow) &= \frac{1}{4}N_c s^2 \beta^2 \sin^2 \theta [D_t + D_u + D_s]^2 (F_2 \mp 1)^2, \\
|\mathcal{M}|^2(\gamma_R\gamma_R \rightarrow t_\uparrow\bar{t}_\uparrow \text{ or } t_\downarrow\bar{t}_\downarrow) &= \frac{1}{4}N_c s^2 (1 - \beta^2) [D_t + D_u]^2 (1 \mp \beta \cos \xi)^2, \\
|\mathcal{M}|^2(\gamma_R\gamma_R \rightarrow t_\uparrow\bar{t}_\downarrow \text{ or } t_\downarrow\bar{t}_\uparrow) &= \frac{1}{4}N_c s^2 \beta^2 (1 - \beta^2) [D_t + D_u]^2 \sin^2 \xi,
\end{aligned} \tag{7}$$

where N_c is the number of color, $D_{s,t,u}$ are the effective propagation factors defined by

$$D_t = \frac{(Q_t e)^2}{t - m_t^2}, \quad D_u = \frac{(Q_t e)^2}{u - m_t^2}, \quad D_s = \frac{4s\lambda}{M_S^4}, \tag{8}$$

and $F_{1,2}$ are the spin configuration factors as functions of the scattering angle, given by

$$\begin{aligned}
F_1 &= \sqrt{1 - \beta^2} \sin \theta \cos \xi - \cos \theta \sin \xi, \\
F_2 &= \sqrt{1 - \beta^2} \sin \theta \sin \xi + \cos \theta \cos \xi.
\end{aligned} \tag{9}$$

The SM results are in agreement with those of Ref. [10]. It has been noted that the processes $\gamma_R\gamma_L \rightarrow (t_\uparrow\bar{t}_\uparrow \text{ or } t_\downarrow\bar{t}_\downarrow)$ permit a special top spin basis where the SM prediction vanishes. The other amplitudes can be obtained by using the CP invariance such as

$$|\mathcal{M}_{RL\uparrow\uparrow}| = |\mathcal{M}_{LR\downarrow\downarrow}|, \quad |\mathcal{M}_{RR\uparrow\downarrow}| = |\mathcal{M}_{LL\downarrow\uparrow}|, \tag{10}$$

where, e.g., the suffix $RL \uparrow\uparrow$ denotes the process $\gamma_R\gamma_L \rightarrow t_\uparrow\bar{t}_\uparrow$.

The squared amplitudes in Eq. (7) imply important characteristic features of the $\gamma\gamma \rightarrow t\bar{t}$ process. First the low scale quantum gravity effects contained in D_s exist only in the $J_z = 2$ cases, as discussed before. Second the effects in any top spin basis do not modify the top spin configuration. This is not the case at e^+e^- colliders: for instance the quantum gravity leads to non-zero observables for like-spin states of the top quark pair in a special spin basis where the SM prediction vanishes [7].

In order to draw the information of large extra dimensions from the top spin configuration, we take notice of the following points: the quantum gravity effects, even being factored out from the spin configuration, appear in the $J_z = 2$ cases, not in the $J_z = 0$ cases; each squared amplitude in Eq. (7) has different top spin configuration factors according to the photon polarization. Hence a combination of the $J_z = 2$ and $J_z = 0$ states

enables low scale quantum gravity to modify the top spin configurations. In fact finite mixing of two photon states is inevitable from the practical point of view, as shall be discussed below. On the other hand, this mixing contaminates the SM prediction of the suppression, in a special top spin basis, of $\gamma_R\gamma_L \rightarrow (t_\uparrow\bar{t}_\uparrow \text{ or } t_\downarrow\bar{t}_\downarrow)$.

We briefly review the differential cross sections at practical $\gamma\gamma$ colliders [12]. From the head-on collisions between the laser and energetic electron (or positron) beams, high energy polarized photons are produced. When x denotes the fraction of the photon beam energy to initial electron beam energy, i.e., $x = E_\gamma/E$, its maximum value is $x_{max} = z/(1+z)$ where $z = 4E\omega_0/m_e^2$. Here E_γ , E , ω_0 are the photon, electron and laser beam energies, respectively. It is known that laser beam with too high energy would produce e^+e^- pair through collisions with the back-scattered photon beam, reducing the $\gamma\gamma$ luminosity. Thus the z is optimized to be $2(1+\sqrt{2})$ which occurs at the threshold for the electron pair production. In the numerical analysis, we consider the following cuts:

$$\begin{aligned} -0.9 &\leq \cos\theta \leq 0.9, \\ \sqrt{0.4} &\leq x_{1(2)} \leq x_{max}|_{z=2(1+\sqrt{2})}. \end{aligned} \quad (11)$$

With given polarizations of the laser and parent electron beams the differential cross section is, taking into account of their Compton back-scattering,

$$\begin{aligned} \frac{d\sigma}{d\cos\theta} &= \frac{1}{32\pi s_{ee}} \int \int dx_1 dx_2 \frac{f(x_1)f(x_2)}{x_1 x_2} \\ &\times \left[\left(\frac{1 + \xi_2(x_1)\xi_2(x_2)}{2} \right) |\mathcal{M}_{J_z=0}|^2 + \left(\frac{1 - \xi_2(x_1)\xi_2(x_2)}{2} \right) |\mathcal{M}_{J_z=2}|^2 \right], \end{aligned} \quad (12)$$

where

$$\begin{aligned} |\mathcal{M}_{J_z=0}|^2 &= \frac{1}{2} \left[|\mathcal{M}_{RR}|^2 + |\mathcal{M}_{LL}|^2 \right], \\ |\mathcal{M}_{J_z=2}|^2 &= \frac{1}{2} \left[|\mathcal{M}_{RL}|^2 + |\mathcal{M}_{LR}|^2 \right]. \end{aligned} \quad (13)$$

And $f(x)$ and $\xi_2(x)$ are the photon number density and the averaged circular polarization of the back-scattered photon beams, respectively, both of which depend on the polarizations of the laser and electron beams [11,13,14]. As $f(x)$ implies, the back-scattered

photons possess non-trivial energy spectrum, which renders unavoidable finite mixing of the $J_z = 2$ and $J_z = 0$ states. The s_{ee} is the CM squared energy at e^+e^- collisions, related with that of $\gamma\gamma$ collisions, s , by $s = x_1x_2s_{ee}$. Since the $\gamma\gamma$ luminosity spectrum shows a narrow peak at around x_{max} with an appropriate cut on the longitudinal momentum of the back-scattered photons [12], the approximations such as $t = x_1x_2t_{ee}$ and $u = x_1x_2u_{ee}$ are to be employed [11,13,14].

III. RESULTS

We estimate various observables of the top quark pair production at photon colliders. Let us first observe that top spin information with CP invariance permits only two independent cross sections,

$$\sigma_{\uparrow\uparrow}(= \sigma_{\downarrow\downarrow}), \quad \sigma_{\uparrow\downarrow}(= \sigma_{\downarrow\uparrow}), \quad (14)$$

which can be easily seen from Eqs. (10) and (13). In Fig. 3, we present $\sigma_{\uparrow\uparrow}$ and $\sigma_{\uparrow\downarrow}$ with respect to $\cos\xi$ at $\sqrt{s_{ee}} = 1$ TeV with unpolarized and/or polarized initial beams. The polarizations of the laser and electron beams are allowed as 100% and 90%, respectively. The M_S is set to be 2.5 TeV. The convex curves denote the $(t_{\uparrow}\bar{t}_{\downarrow})$ case, while the concave ones do the $(t_{\uparrow}\bar{t}_{\uparrow})$ case. The solid lines describe the SM results, and the dotted and dashed lines describe the results including low scale quantum gravity effects with $\lambda = 1$ and $\lambda = -1$, respectively. Each value of $\cos\xi$ indicates different spin basis of the top quark and anti-quark.

There are several interesting characteristics of photon colliders in producing top quark pair. As can be first seen in Fig. 3, there is no special $\cos\xi$ at which one top spin configuration dominates over the other, as discussed before. The quantum gravity effects manifest themselves as being factored out from the top spin configuration, i.e., independent of $\cos\xi$. And irrespective of the polarizations of the laser and electron beams, the effects are larger in the cases of $t_{\uparrow}\bar{t}_{\downarrow}$ than in those of $t_{\uparrow}\bar{t}_{\uparrow}$. Equation (7) suggests its reason.

For instance, with the unpolarized beams, the ratio $|\mathcal{M}_{RL}/\mathcal{M}_{RR}|^2$ hints the magnitude of the quantum gravity effects, since the $J_z = 2$ states possess the effects but the $J_z = 0$ states do not. Hence the top quark pair production channel with the $(t_{\uparrow}\bar{t}_{\downarrow})$ is effective to probe the quantum gravity effects. Finally we observe that the results with the polarized electron beams are of great interest and importance: there exist two values of $\cos\xi$, i.e., two special spin bases where the equalities $\sigma_{\uparrow\uparrow} = \sigma_{\uparrow\downarrow}$ hold true as shown in Fig. 3 (c) and (d). Considering a new observable, top spin asymmetry A^{top} ,

$$A^{top} = \frac{\sigma_{\uparrow\downarrow} - \sigma_{\uparrow\uparrow}}{\sigma_{\uparrow\downarrow} + \sigma_{\uparrow\uparrow}}, \quad (15)$$

we suggest an optimal top spin basis defined by ξ_0 which satisfies

$$\sigma_{\uparrow\downarrow}^{SM}(\xi_0) = \sigma_{\uparrow\uparrow}^{SM}(\xi_0). \quad (16)$$

The definition guarantees that the observable $A^{top}(\xi_0)$ vanishes in the SM while retains non-vanishing values with the low scale quantum gravity effects. The $A^{top}(\xi_0)$ as a function of M_S is plotted in Fig. 4. The solid lines indicate the SM predictions at 2σ level, while the dotted and dashed lines include the quantum gravity effects of $\lambda = 1$ and $\lambda = -1$, respectively. The case of $M_S = 2.5$ TeV at $\sqrt{s_{ee}} = 1.0$ TeV causes about $A^{top}(\xi_0)$ of 6%.

$(P_{e1}, P_{e2}, P_{l1}, P_{l2})$	σ_{tot}		$\sigma_{\uparrow\uparrow}$		$\sigma_{\uparrow\downarrow}$	
	$\lambda = 1$	$\lambda = -1$	$\lambda = 1$	$\lambda = -1$	$\lambda = 1$	$\lambda = -1$
(0,0,0,0)	4.1	4.1	2.6	2.8	4.3	4.3
(0,0,1,1)	4.0	4.0	2.5	2.7	4.2	4.2
(0.9,0.9,0,0)	3.2	3.2	1.7	2.0	3.7	3.7
(0.9,0.9,1,1)	3.2	3.2	1.8	2.0	3.5	3.6

Table I. The photon collider bounds of M_S in TeV at 2σ level according to the polarizations of the laser, the parent electron beam, and top spin configurations.

The $A^{top}(\xi_0)$ observables yield lower bounds on the string scale M_S , which can be read off from Fig. 4. In Table I, we summarize other lower bounds of the M_S , which can

be obtained by using various combination of the polarizations of the laser and electron beams, and by measuring the top spin configuration. We have employed the luminosity $\mathcal{L} = 200\text{fb}^{-1}$. As discussed before, the top spin state $(t_{\uparrow}\bar{t}_{\downarrow})$ can constrain most strictly the M_S , though the enhancement of the M_S bound is not very significant. This is mainly due to the statistical disadvantage of the top spin measurements.

IV. CONCLUSIONS

The experimental feasibility of the determination of top spin configuration and construction of high energy linear photon colliders provides a new window to probe physics beyond the standard model. We have studied top pair production at $\gamma\gamma$ linear colliders with the large extra dimension effects. From the polarized scattering amplitudes in a general top spin basis, it has been shown that only the $J_z = 2$ states receive the effects, which do not affect the top spin configuration. The non-trivial energy spectrum of the Compton back-scattered photons leads to finite mixing of the $J_z = 0$ and $J_z = 2$ states, as well as permitting low scale quantum gravity to play a role in modifying the top spin configuration. Considering the Compton scattering also, total cross sections in a general top spin basis have been presented; the large extra dimension effects are shown to be larger for the $(t_{\uparrow}\bar{t}_{\downarrow})$ configuration than for the $(t_{\uparrow}\bar{t}_{\uparrow})$ one. On the other hand, this practical mixing of the $J_z = 0$ and $J_z = 2$ states is shown to eliminate the presence of a top spin basis in which one of the final spin configurations is dominant and the other suppressed. Instead we have noticed that a special spin basis, especially with the polarized parent electron beams, exist such that $\sigma^{SM}(t_{\uparrow}\bar{t}_{\downarrow}) = \sigma^{SM}(t_{\uparrow}\bar{t}_{\uparrow})$ in the SM. Accordingly introduced is the top spin asymmetry A^{top} of which the SM predictions vanish in this optimal top spin basis, which can be one of the most effective tools. Low scale quantum gravity at $\sqrt{s_{ee}} = 1$ TeV with the string scale $M_S = 2.5$ TeV predicts about 6% of A^{top} in the optimal top spin basis. From various observables, we have also estimated the lower bounds of the M_S in the range of 1.7 to 4.3 TeV, summarized in Table I. The measurements of the top spin

configuration as $(t_{\uparrow}\bar{t}_{\downarrow})$ improve the lower bounds for M_S more than 200 GeV.

ACKNOWLEDGMENTS

This work is supported in part by the Korean Science and Engineering Foundation (KOSEF) through the Center for Theoretical Physics (CTP) at Seoul National University.

REFERENCES

- [1] N. Arkani-Hamed, S. Dimopoulos, and G. Dvali, Phys. Lett. B **429**, 263 (1998); Phys. Rev. D **59**, 086004 (1999); I. Antoniadis, N. Arkani-Hamed, S. Dimopoulos, and G. Dvali, Phys. Lett. B **436**, 257 (1998).
- [2] T. Han, J.D. Lykken, and R.-J. Zhang, Phys. Rev. D **59**, 105006 (1999); G.F. Giudice, R. Rattazzi, and J.D. Wells, Nucl. Phys. **B544**, 3 (1999).
- [3] E.A. Mirabelli, M. Perelstein, and M.E. Peskin, Phys. Rev. Lett. **82**, 2236 (1999); K. Cheung and W. Keung, hep-ph/9903294; I. Antoniadis, K. Benakli, and M. Quirós, hep-ph/9905311; M. Besançon, hep-ph/9909364; D. Atwood, S. Bar-Shalom, and A. Soni, hep-ph/9909392.
- [4] J.L. Hewett, Phys. Rev. Lett. **82**, 4765 (1999); T.G. Rizzo, Phys. Rev. D **59**, 115010 (1999); Phys. Rev. D **60**, 075001 (1999); A.K. Gupta, N.K. Mondal, and S. Raychaudhuri, hep-ph/9904234; K. Agashe and N.G. Deshpande, Phys. Lett. B **456**, 60 (1999); P. Mathews, S. Raychaudhuri, and K. Sridhar, Phys. Lett. B **450**, 343 (1999); Phys. Lett. B **455**, 115 (1999); hep-ph/9904232; D. Atwood, S. Bar-Shalom, and A. Soni, hep-ph/9903538; C. Balázs, H.-J. He, W.W. Repko, C.-P. Yuan, and D.A. Dicus, Phys. Rev. Lett. **83**, 2112 (1999); K.Y. Lee, H.S. Song, and J. Song, hep-ph/9904355; K. Cheung, hep-ph/9904266; Phys. Lett. B **460**, 383 (1999); S. Mele and E. Sánchez, hep-ph/9909294; K. Cheung and G. Landsberg, hep-ph/9909218; O.J.P. Éboli, T. Han, M.B. Magro, and P.G. Mercadante, hep-ph/9908358; D.K. Ghosh, P. Poullose, and K. Sridhar, hep-ph/9909377.
- [5] F. Abe *et. al.*, CDF Collaboration, Phys. Rev. Lett. **74** 2626 (1995); Phys. Rev. D **50**, 2966 (1994).
- [6] T. Arens and L.M. Sehgal, Nucl. Phys. **B393**, 46 (1993); Phys. Rev. D **50**, 4372 (1994); G. Mahlon and S. Parke, Phys. Rev. D **53**, 4886 (1996).

- [7] K.Y. Lee, H.S. Song, J. Song, and C. Yu, Phys. Rev. D **60**, 093002 (1999).
- [8] T. G. Rizzo, hep-ph/9904380; X. He, hep-ph/9905295; P. Mathews, P. Poulose, and K. Sridhar, hep-ph/9905395; D.K. Ghosh, P. Mathews, P. Poulose, and K. Sridhar, hep-ph/9909567.
- [9] S. Parke and Y. Shadmi, Phys. Lett. B **387**, 199 (1996); S. Parke, hep-ph/9807573; J. Kodaira, T. Nasuno, and S. Parke, Phys. Rev. D **59**, 014023 (1999).
- [10] M. Hori, Y. Kiyo, and T. Nasuno, Phys. Rev. D **58**, 014005 (1998);
- [11] J. Choi, S.Y. Choi, S.H. Ie, and H.S. Song, Phys. Rev. D **36**, 1320 (1987).
- [12] I.F. Ginzburg, G.L. Kotkin, V.G. Serbo, and V.I. Telnov, Nucl. Instr. and Meth. **205**, 47 (1983); I.F. Ginzburg, G.L. Kotkin, S.L. Panfil, V.G. Serbo, and V.I. Telnov, Nucl. Instr. and Meth. **219**, 5 (1984); V.I. Telnov, hep-ex/9908005; hep-ex/9910010.
- [13] H. Davoudiasl, Phys. Rev. D **60**, 084022 (1999).
- [14] S.Y. Choi, K. Hagiwara, and M.S. Baek, Phys. Rev. D **54**, 6703 (1996); M.S. Baek, S.Y. Choi, and C.S. Kim, Phys. Rev. D **56**, 6835 (1997).

Figure Captions

Fig. 1 : Feynman diagrams for the $\gamma\gamma \rightarrow t\bar{t}$ process with the large extra dimension effects.

Fig. 2 : The generic spin basis: (a) in the top quark rest frame; (b) in the top anti-quark rest frame.

Fig. 3 : Total cross sections as a function of $\cos\xi$: (a) with the unpolarized beams, i.e., $(P_{e1}, P_{e2}, P_{t1}, P_{t2}) = (0, 0, 0, 0)$; (b) $(0, 0, 1, 1)$; (c) $(0.9, 0.9, 0, 0)$; (d) $(0.9, 0.9, 1, 1)$. The convex curves denote the $(t_{\uparrow}\bar{t}_{\downarrow})$ case, while the concave ones do the $(t_{\uparrow}\bar{t}_{\uparrow})$ case. The solid lines describe the SM results, and the dotted and dashed lines describe the results including low scale quantum gravity effects with $\lambda = 1$ and $\lambda = -1$, respectively.

Fig. 4 : The optimal top spin asymmetries with respect to M_S with unpolarized and/or polarized initial beams. The solid lines denote 2σ level predictions of the SM. The dotted and dashed lines incorporate low scale quantum gravity effects in the cases of $\lambda = 1$ and $\lambda = -1$, respectively.

FIGURES

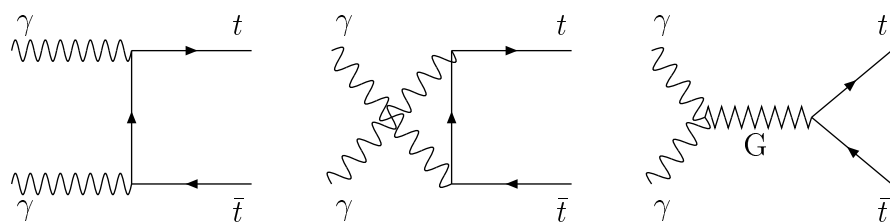


Fig. 1

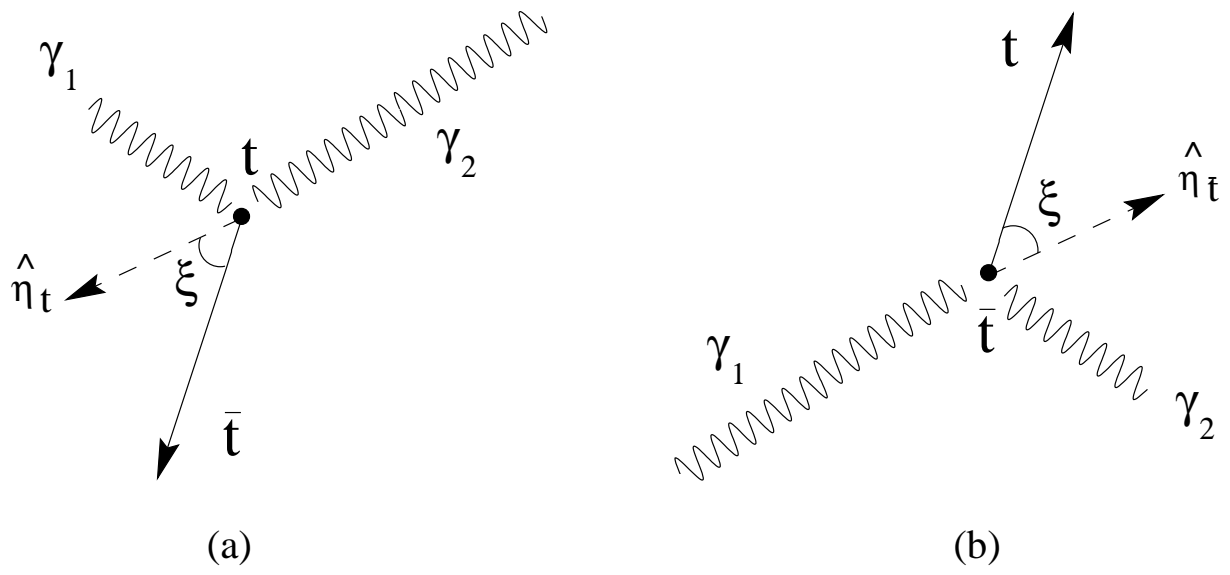


Fig. 2

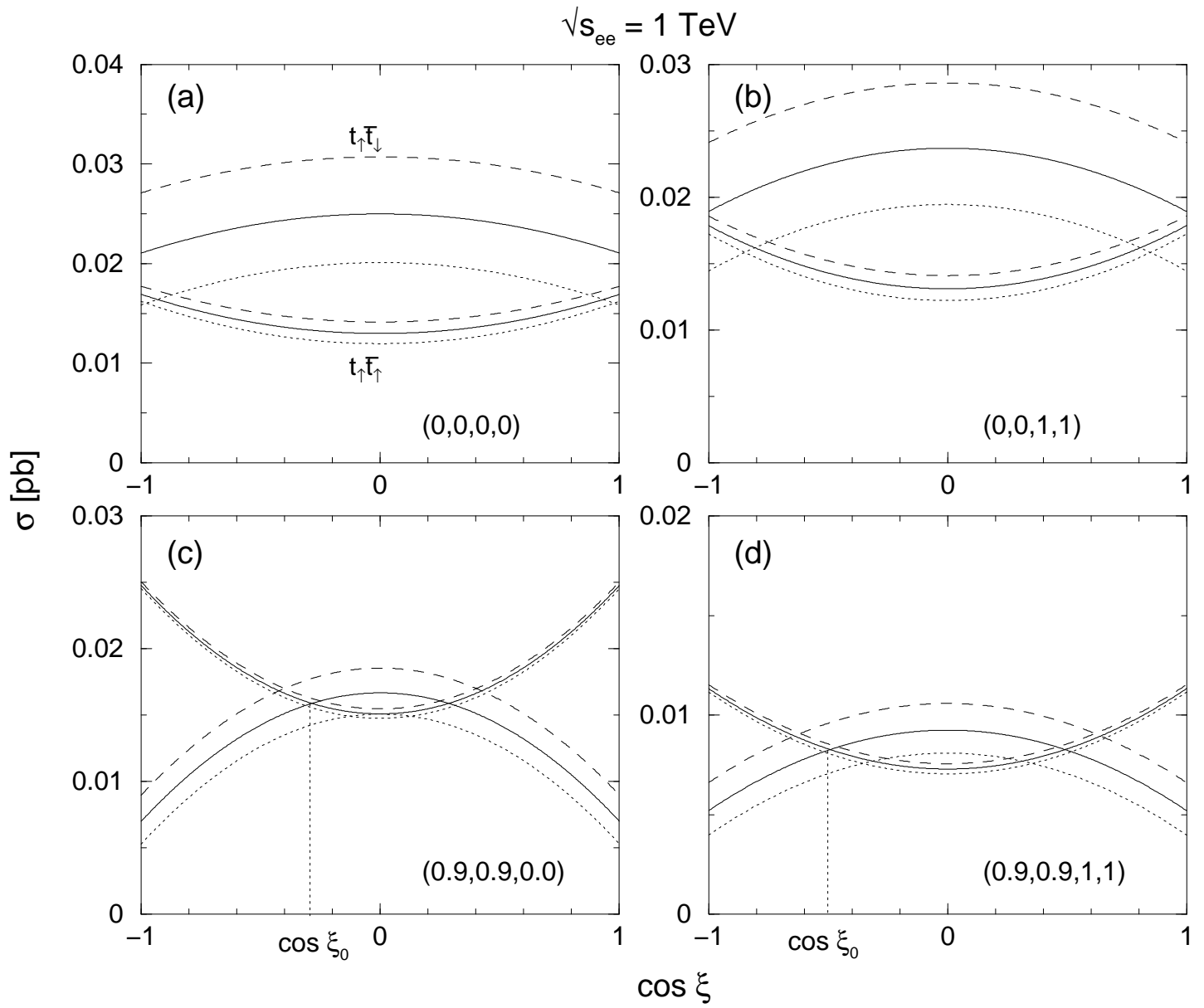


Fig. 3

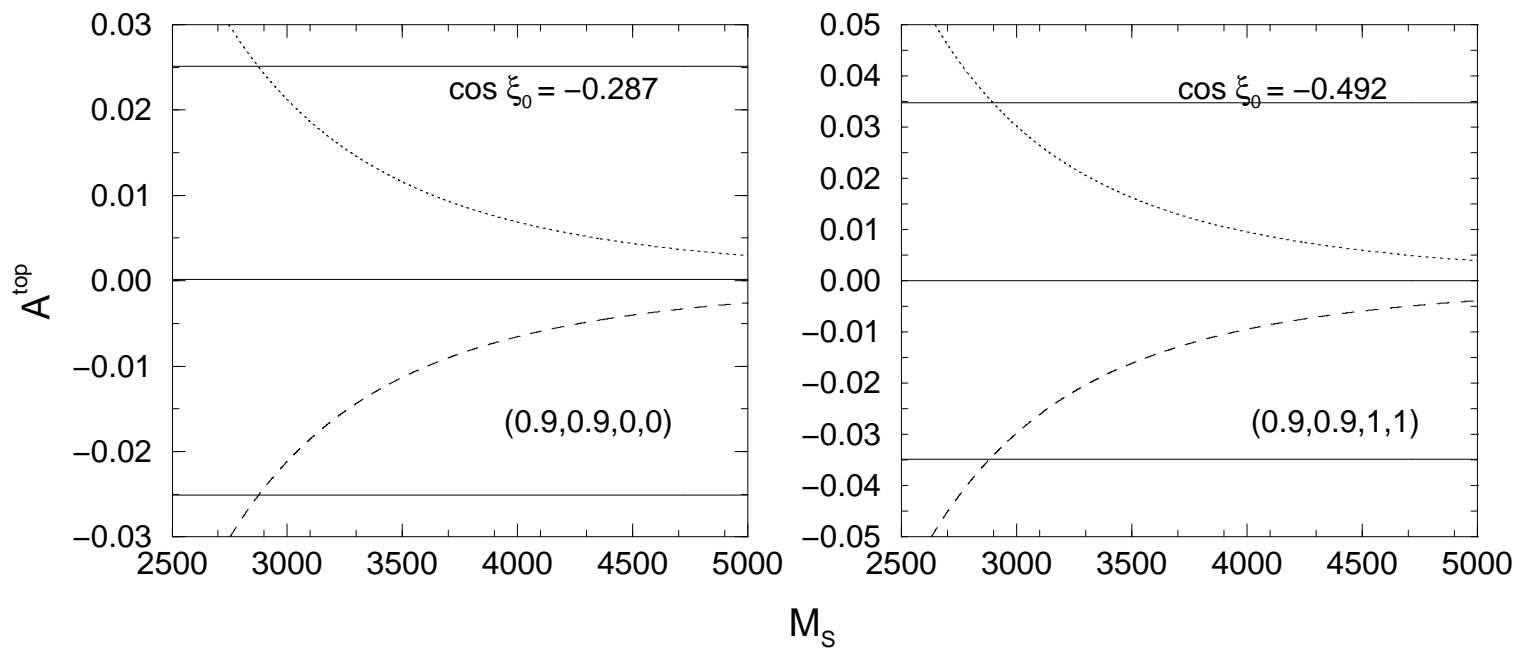


Fig. 4